# Engineering Approximations for Radiating Nonequilibrium Shock Layers

LELAND A. CARLSON*
*Texas A&M University, College Station, Texas*

**An approximate analytic solution for rapidly obtaining engineering solutions for radiating reacting 14–18 km/sec air normal shock waves is presented. Near the shock front first ionization nonequilibrium is included, and the dominant radiative transfer is assumed to be from spectral regions having large absorption coefficients. Downstream, equilibrium is assumed and radiative cooling due to transparent emission is permitted. The solution near the shock front indicates that the flow is primarily chemistry dominated, that radiative losses in the nonequilibrium zone can affect the entire flowfield, and that conduction can be significant.**

## Introduction

THE flowfield behind a hypervelocity shock wave involves chemically reacting species and radiative transfer. For those cases where the shock layer is in chemical equilibrium, many excellent analysis techniques have been developed; and these have been summarized in a survey article by Anderson.[1] At high altitudes, however, chemical and thermal nonequilibrium phenomena become important along with radiative and possibly conductive effects. Detailed solutions of such complicated flowfields are extremely difficult, require extensive computational effort, and are from a practical standpoint limited to a few specific cases.[2-4] Adequate engineering design optimization of advanced hypervelocity vehicles will require, however, a large number of parametric calculations; and hence rapid, reasonably accurate solution techniques for nonequilibrium radiating shock layers would be desirable.

The objectives of this paper are to investigate various approximations that can be used in analyzing radiating reacting shock layers, to develop a rapid solution technique that is suitable for initial design, parametric, and optimization studies, and, in so doing, to uncover important features of such flows. It should be noted that the approximations discussed in this paper need not always be applied simultaneously. Also the resultant techniques are applied to normal shock flows only to simplify discussion. All of them can, in principle, be extended to multi-dimensional and entry vehicle flowfields.

## Semidetailed Numerical Solution

The primary equations governing the radiating reacting flow behind a hypervelocity shock wave are the global energy equation, Eq. (1)

$$\rho u \frac{dh}{dx} + \frac{d}{dx}\left[\sum_{i=1}^{s}\left(-\lambda_i \frac{dT_i}{dx}\right)\right] + \frac{d}{dx}\left[\sum_{i=1}^{s} \rho_i U_i h_i\right] + \frac{d\dot{q}_R}{dx} - u\frac{dp}{dx} = -\sum_{i=1}^{s} \dot{w}_i h_i^0 \quad (1)$$

and the equation of radiative transfer. If the flow is assumed to be one-dimensional and if the nongray absorption coefficient is represented by a series of gray gas steps, the latter can be expressed as

$$\dot{q}_R(x) = 2\pi \sum_i \int_0^{\tau_{cs_i}} [\operatorname{sgn}(\tau_i - z_i)] S_i(z_i) E_2(|\tau_i - z_i|)\, dz_i \quad (2)$$

where the summation is over the spectral regions of the step model and $\tau_i$ is the optical thickness at point $x$ for region $i$. Normally these equations must be solved in conjunction with the conservation equations for species mass, momentum, and electron energy, etc., and because the radiative transfer depends upon the flowfield solution, some type of iteration on the entire flowfield must be performed. Local iteration to determine the electron temperature is also usually required. With the introduction of chemical nonequilibrium, many flowfield points must be calculated in the immediate postshock region in order to adequately represent the large temperature and species concentration gradients; and this fact coupled with the requirement for iteration frequently results in large computer times. Consequently, any simplification in the representation of the radiative transfer term or in the method of calculating the electron temperature would be valuable.

An examination of two-temperature solutions (i.e., heavy particle temperature unequal to electron temperature) reveals that the electron temperature is relatively constant throughout much of the relaxation zone.[2-5] Consequently, one possible approximation is to represent the electron temperature in the relaxation zone by some selected constant value or the heavy particle temperature, whichever is lower. This approach, which has been successfully used,[6] eliminates the electron energy equation and its associated iteration and significantly reduces the computational effort required.

Many approximations to the energy equation radiative transfer term have been utilized in the past.[1] For the most part, these have assumed the gas to be either transparent or gray; or in the general case they have represented the nongray absorption coefficient by a series of gray gas steps. While making radiative flowfield problems at least tractable, these approximations by themselves still result in the nonequilibrium case in extensive computer times. As a consequence, this author and Skoczlas[7] investigated further approximations appropriate to the nonequilibrium situation.

In the relaxation zone the primary radiative losses originate from those spectral regions having large absorption coefficients, $K_i$, and the corresponding optical thickness

$$\tau_i = \int_0^x K_i\, dx$$

is also large. Thus, the exponential integral function, $E_2$, in Eq. (2) rapidly approaches zero away from the point in question, and only the region near a point affects the radiative transfer at a point. By assuming that in this region the source function, $S_i(x)$, is essentially constant and that the optical thickness can

Presented as Paper 73-673 at the AIAA 6th Fluid and Plasma Dynamics Conference, Palm Springs, Calif., July 16–18, 1973; submitted July 24, 1973; revision received December 6, 1973.

Index categories: Radiatively Coupled Flows and Heat Transfer; Shock Waves and Detonations.

* Assistant Professor, Aerospace Engineering Department. Member AIAA.

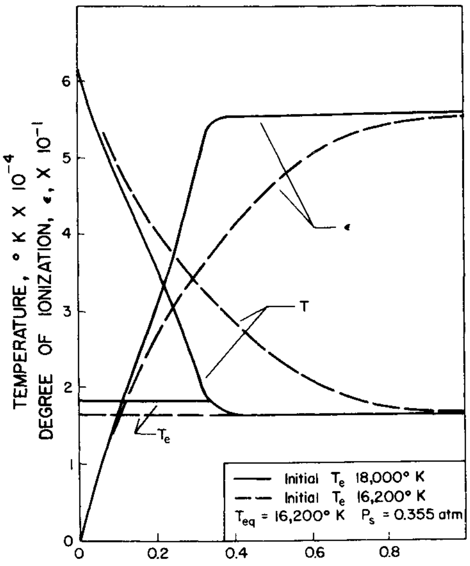


**Fig. 1 The effect of electron temperature on shock layer profiles (nitrogen).**

be approximated by $\tau_i(x) = K_i(x)x$, Eq. (2) can be approximated as

$$\dot{q}_R = 2\pi \sum_i [\![S_i(x)\{E_3[K_i(x)(x_{cs}-x)] - E_3[K_i(x)\cdot x]\}]\!] \quad (3)$$

where $x_{cs}$ is the location of a downstream contact surface (for example, the interface between the driver and driven gas in a shock tube). Notice that in Eq. (3) the source function, $S_i$, and the absorption coefficient are still functions of $x$ since they depend upon the local temperature and composition. Also, as can be seen this approximation yields the radiative transfer at each point as a function only of the properties at the point, and thus it eliminates the iterative nature of the radiative transfer calculation. Since radiative transfer is not expected to dominate the relaxation zone, this approximation may be quite adequate for the nonequilibrium part of the flowfield.

In applying the abovementioned method, previously determined and experimentally verified radiative cross sections, $\sigma_i$, for equilibrium flows[8] can be utilized if they and the corresponding source function are appropriately modified for nonequilibrium effects. For photoionization from the ground state the appropriate source function and absorption coefficient are[2-4]

$$S = \frac{\varepsilon^2}{1-\varepsilon}\frac{1-\varepsilon_e}{\varepsilon_e^2}\int_0^{852} B_\lambda \, d\lambda \quad (4a)$$

$$K_i = N_A \sigma_i \quad (4b)$$

where $N_A$ is the local atom concentration, $\sigma_i$ is an average radiative cross section for the spectral region in question and $\varepsilon$ is the degree of ionization. The symbol $\varepsilon_e$ is the degree of ionization which would exist if the flow were in equilibrium at the local pressure and electron temperature. For those regions involving photoionization from excited states in thermal equilibrium at the local electron temperature, $T_e$, the source function is simply the integrated black body function, and the absorption coefficients can be based upon equilibrium cross sections if

$$K_i = \frac{\varepsilon^2}{1-\varepsilon}\frac{1-\varepsilon_e}{\varepsilon_e^2} N_A \sigma_i \quad (5)$$

For spectral regions involving only line radiation, no correction is required if local concentrations and temperatures are used.

This entire method was applied to inviscid normal shock flows by Skoczlas[7] using a two-step radiation model and shown to yield reasonably accurate solutions for nonequilibrium nitrogen in about 1/500th the time required for detailed solutions. Skoczlas, however, did not include in his chemistry model the effects of photoionization, which may be important as equilibrium is approached.[3] Some new results for nitrogen using the above approximations are shown in Figs. 1 and 2. These results include collisional and photoionization chemistry, not only from the ground state but also from excited states, and utilize a five-step nonequilibrium absorption coefficient model. In addition a precursor degree of ionization level of $10^{-3}$ was assumed in accord with experimental observation, and dissociation was considered to be complete in the shock front.[9]

As indicated previously the electron temperature is approximated in the relaxation zone by a constant value. Since both the radiative transfer and the species rate of production depend upon electron temperature,[5] this value must be selected carefully. Figure 1 shows the effect of the assumed value of electron temperature on the relaxation zone for the case where the radiation is uncoupled from the gasdynamics. The important item to notice is that a small increase in the average electron temperature results in a factor of three decrease in the relaxation zone length. Since experimental evidence indicates that relaxation distances in air are very short,[9] these results demonstrate that the average value of $T_e$ should probably be selected at a value several thousand degrees above the ideal Rankine-Hugoniot equilibrium temperature.

Figure 2 shows results for the same nitrogen normal shock wave but with radiation coupled to the gasdynamics via Eqs. (3–5). Notice that the photoionization rate, $\dot{w}_{e,\text{rad}}$, never dominates the nonequilibrium chemistry and that in approximate calculations it could probably be ignored. Further, the heavy particle temperature in this radiatively cooled case decreases more rapidly than the corresponding uncoupled radiation prediction (Fig. 1) and reaches the ideal equilibrium temperature in about half the distance. Obviously, these semidetailed solutions demonstrate that while chemistry dominates the relaxation zone, there is still significant radiative cooling and radiative-chemistry coupling occurring.

Even though this semidetailed approach can yield accurate answers and reveal important phenomena with reduced computational effort, it still requires a significant amount of time for even simple normal shock cases (30 sec, IBM 360/65). Further, due to the approximations inherent in Eq. (3), it does not treat the equilibrium portion of the flowfield efficiently; and it is of sufficient complexity so as to limit parametric type studies.

## Development of Approximate Solution

Based upon previous detailed solutions[2-5] and the semidetailed solutions obtained in this study, several significant

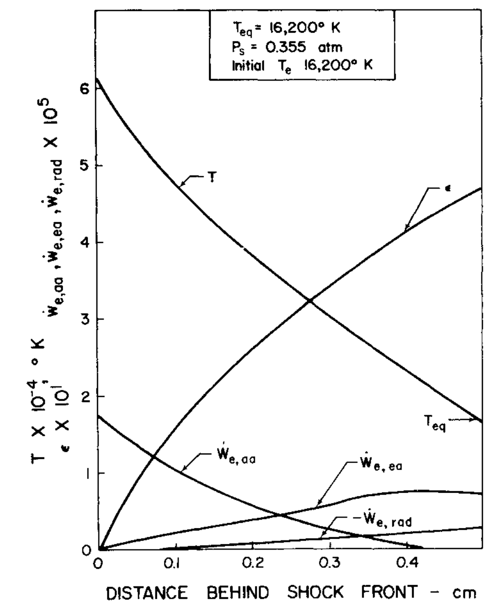


**Fig. 2 Shock layer profiles in nitrogen (semidetailed solution).**

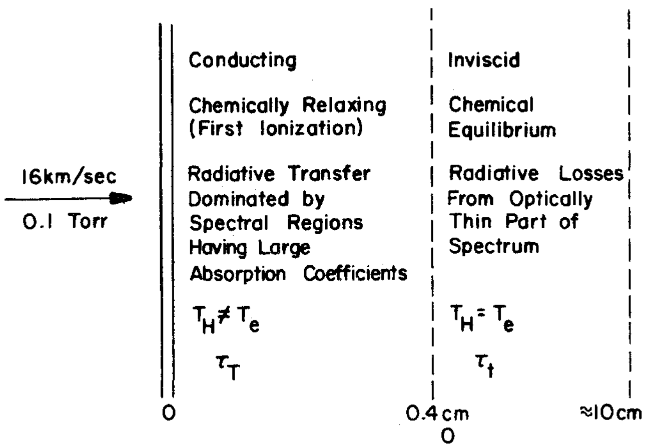


**Fig. 3 Hypervelocity normal shock structure.**

features of air radiating reacting hypervelocity shock layers in the 12–18 km/sec range were determined; and these are schematically represented on Fig. 3. Typically the shock layer is composed of a short chemical relaxation zone immediately behind the shock front that is dominated by first ionization since dissociation is complete in the shock front.[5,9] In this region the electron temperature is not equal to the heavy particle temperature, and most of the radiative losses occur from the ultraviolet, which is characterized by large absorption coefficients. Also, large temperature gradients exist in this region and thermal conduction should be important. Downstream the flowfield is inviscid, in chemical and thermal equilibrium, and experiences radiative energy losses from essentially only the transparent visible portion of the spectrum, which is characterized by small absorption coefficients.

Based upon the origin of the radiative losses, it was decided to represent the radiative transfer by a thick-transparent approximation similar to that suggested and formalized by Olstad.[10] This approach includes, at a point, only that part of the spectrum contributing significantly to radiative cooling. Thus, for the nonequilibrium relaxation region, the solution depends upon the radiative transfer from only those regions having large absorption coefficients. Since regions having large absorption coefficients are frequently referred to as being optically thick, the relaxation portion of the flowfield will subsequently be referred to as the thick region and it will be characterized by the corresponding optical thickness coordinate, $\tau_T$. Likewise, the downstream equilibrium region will only include transparent radiation losses (which have small absorption coefficients), will be denoted as the thin region, and will be characterized by the optical thickness, $\tau_t$, associated with the thin part of the spectrum. With this approach, solutions for each region can be obtained separately; and the downstream result for the thick region can serve as the upstream boundary condition for the thin region. This approach has been used in the past for equilibrium[10] and for frozen shock layers,[11] and a related layering approach has been used for nonconducting nonequilibrium flows.[4]

Assuming dissociation complete in the shock front, ambipolar diffusion, and constant postshock pressure, and with $h = c_p(T + \varepsilon T_e)$, Eq. (1) becomes after nondimensionalizing all flow properties by the appropriate inviscid postshock value and distance by a reference length $L$

$$\bar{\rho}\bar{u}\frac{d\bar{h}}{d\bar{x}} - (Re)^{-1}\frac{d}{d\bar{x}}\left(\frac{\bar{\mu}}{Pr}\frac{d\bar{h}}{d\bar{x}}\right) + Re^{-1}\bar{h}_e\frac{d}{d\bar{x}}\left(\frac{\bar{\mu}}{Pr}\frac{d\varepsilon}{d\bar{x}}\right) = -(\rho_s u_s h_s)^{-1}\frac{d\dot{q}_R}{d\bar{x}} - (\bar{h}_I{}^0 - \bar{h}_A{}^0)\bar{\rho}\bar{u}\frac{d\varepsilon}{d\bar{x}} \qquad (6)$$

where bars denote nondimensional variables, $Re = \rho_s u_s L/\mu_s$, $\bar{h}_e = c_p T_e/h_s$, and $\bar{h}_i{}^0$ is the zero point enthalpy of species $i$. Notice that thermal conduction, radiative transfer, and chemical and thermal nonequilibrium have been included.

By transforming, first using $d\bar{n} = \bar{\rho}\, d\bar{x}$ and then $d\tau_i = (K_i L/\bar{\rho})\, d\bar{n}$, and by assuming $\bar{\rho}\bar{\mu}$ one and constant Prandtl number, Eq. (6) becomes

$$\frac{d\bar{h}}{d\tau_i} - \frac{K_i L}{\bar{\rho}\, Re\, Pr}\frac{d^2\bar{h}}{d\tau_i{}^2} + \frac{K_i L}{\bar{\rho}\, Re\, Pr}\bar{h}_e\frac{d^2\varepsilon}{d\tau_i{}^2} = \frac{-d\dot{q}_R}{d\bar{x}}(\rho_s u_s h_s K_i L)^{-1} - (\bar{h}_I{}^0 - \bar{h}_A{}^0)\frac{d\varepsilon}{d\tau_i} \qquad (7)$$

For the region near the shock front (denoted by subscript $T$), it is assumed that $K_T = K_{Ts}\bar{\rho}$, where $K_{Ts}$ is the absorption coefficient of region $T$ evaluated immediately behind the shock front. This assumption corresponds to assuming a constant absorption cross section for the region, and yet it retains via $\bar{\rho}$ the dependence of $K_T$ upon the flow properties and hence upon $x$. Next, for a gray gas step $i$

$$\frac{-d\dot{q}_{Ri}(\tau_i)}{dx} = -4\pi K_i S_i + 2\pi K_i \int_0^\infty S_i E_1(\tau_i - z_i)\, dz_i \qquad (8)$$

For the thick region, $E_1(x)$ can be replaced by the exponential approximation $2\exp(-2x)$, and the regional source function $S_i$ can be considered constant at the shock value $S_{Ts}$, since the electron temperature is assumed constant in the thick region and only the region near $\tau_i$ contributes to the integral. Hence, for the thick region

$$\frac{-d\dot{q}_{R_T}}{dx} = -2\pi K_T S_{Ts}\exp(-2\tau_T) \qquad (9)$$

It should be noted that Eq. (9) is not an optically thick or diffusion approximation. Instead, it is an expression based upon the properties of the spectral region dominating the radiative transfer near the shock front, and it corresponds to Olstad's first-order thick approximation evaluated near a boundary.[10]

Now to solve Eq. (7) the degree of ionization, $\varepsilon$, must be known, and for the thick region it can be approximated as

$$\varepsilon = \varepsilon_{eq}[1 - \exp(-B\tau_T)] \qquad (10)$$

where $\varepsilon_{eq}$ is the downstream equilibrium condition and $B$ is determined by correlation with experimental relaxation data. This form is based upon detailed[2–5] and semidetailed[6,7] results, and it will yield phenomenologically correct profiles. The important point is that it uncouples the species production and energy equations and permits a solution of the latter.

Thus, for the thick region near the shock front, Eq. (7) becomes

$$A\bar{h}'' - \bar{h}' = \Gamma_T\exp(-2\tau_T) + C\exp(-B\tau_T) \qquad (11)$$

where prime denotes differentiation with respect to $\tau_T$ and

$$A = K_{Ts}L/Re\, Pr \qquad \Gamma_T = 2\pi S_{Ts}/\rho_s u_s h_s$$
$$C = (\bar{h}_I{}^0 - \bar{h}_A{}^0)\varepsilon_{eq}B - A\varepsilon_{eq}B^2\bar{h}_e \qquad (12)$$

The appropriate boundary conditions[12,13] for Eq. (11) are at $\tau_T = 0$, $\bar{h} = 1 + A\bar{h}' - A(\bar{h}_e B\varepsilon_{eq})$, and at $\tau_T$ of infinity, $\bar{h} = \bar{h}_0$, which corresponds to complete equilibrium at $\varepsilon_{eq}$. Note that the shock boundary condition not only includes conduction effects but also indirectly includes radiative and chemical effects since it depends upon the form of the solution.

For the downstream region the flow is in complete chemical equilibrium, and for the conditions here of interest the relationship between $\varepsilon$ and $h$ can be closely approximated[14] by

$$\varepsilon = a\bar{h} + b \qquad (13)$$

where $a$ and $b$ are selected so as to fit air thermodynamic data.[14] As in the thick case, this approximation uncouples the equations and permits a solution for $\bar{h}$. Further, if in the thin region (denoted by subscript $t$) it is assumed that the equilibrium absorption coefficient can be represented as $K_t = K_{t0}\bar{\rho}/\bar{\rho}_0$ where subscript 0 denotes conditions at the start of the thin region, then the radiation term can be approximated as

$$d\dot{q}_{R_t}/dx = E_{t0}\rho h^n/\rho_0 h_0{}^n \qquad (14)$$

where $E_{t0}$ is the radiative emission loss at the beginning of thin zone. Thus, for the nonconducting downstream region Eq. (7) becomes

$$[1 + a(\bar{h}_I{}^0 - \bar{h}_A{}^0)]\bar{h}' = -[\Gamma_t/(K_{t0}L)](\bar{h}/\bar{h}_0)^n \qquad (15)$$

where differentiation is respect to $\tau_t$, $\Gamma_t = E_{t0}L/(\rho_s u_s h_s)$, and the boundary condition is $\bar{h} = \bar{h}_0$ at $\tau_t$ zero. (Physically, $\tau_T$ infinity corresponds to $\tau_t$ zero.)

Solutions to Eqs. (11) and (15) are

$$\bar{h}_T = 1 - \tfrac{1}{2}\Gamma_T[1-\exp(-2\tau_T)/(1+2A)] - (\bar{h}_I^0 - \bar{h}_A^0)\varepsilon_{eq} + C\exp(-B\tau_T)/(B+B^2A) \quad (16)$$

$$\bar{h}_t = [\bar{h}_0^{1-n} + (n-1)\Gamma_t\tau_t/(K_{t0}L\bar{h}_0^n F)]^{1/1-n} \quad (17)$$

where

$$\bar{h}_0 = [1 - \tfrac{1}{2}\Gamma_T - b(\bar{h}_I^0 - \bar{h}_A^0)]/F$$
$$F = 1 + a(\bar{h}_I^0 - \bar{h}_A^0) \quad (18)$$

and $\varepsilon_{eq}$ should be based upon $\bar{h}_0$ and Eq. (13).

The physical coordinates can be obtained from the transformations as

$$x_T = (K_{Ts}^{-1})\left\{(1 - \tfrac{1}{2}\Gamma_T - (\bar{h}_I^0 - \bar{h}_A^0)\varepsilon_{eq})\tau_T + \frac{\Gamma_T[1-\exp(-2\tau_T)]}{4+8A} + \frac{C[1-\exp(-B\tau_T)]}{B^2(1+BA)}\right\} \quad (19)$$

$$x_t = LF\bar{h}_0^{n-1}(\bar{h}_t^{2-n} - \bar{h}_0^{2-n})/[\Gamma_t(n-2)] \quad (20)$$

If desired, Eqs. (16) and (17) could be combined into a composite solution.

Once the enthalpy profiles are obtained, it is a simple matter to obtain the radiative heat flux. For example, at the shock front, the radiative flux in the negative $x$-direction is

$$\dot{q}_R(0) = \dot{q}_{R_T}(0) + \dot{q}_{R_t}(0) \quad (21)$$

where from Eq. (9)

$$\dot{q}_{R_T}(0) = -\pi S_{T_s} \quad (22)$$

Likewise, substitution of Eq. (17) into Eq. (14) and integration over the slug of gas being considered yields

$$\dot{q}_{R_t}(0) = \frac{-E_{t0}LF}{2\Gamma_t}[\bar{h}_0 - \bar{h}_t(L)] \quad (23)$$

where $L$ is the length of the gas slug and use is made of the fact that for transparent emission $\dot{q}_{R_t}(0) = -\dot{q}_{R_t}(L)$.

It is believed these are the first solutions to include in a coupled manner the simultaneous effects of nonequilibrium chemistry, nongray nonequilibrium radiation, and thermal conduction. In addition, they are in a form suitable for parametric studies.

## Application of Approximate Solution

In order to obtain solutions several parameters must be known in advance. However, these can be easily obtained by using the procedure indicated on Table 1 and the suggested values given by Figs. 4 and 5. If better estimates of air radiative properties or chemical relaxation lengths are available, they, of course, should be used. In the formula for the chemistry correlation parameter, $B$, on Table 1, the symbols $\bar{h}_2$ denotes the non-

Table 1 Information required to obtain a solution

| Name | Symbols | Recommended source |
|---|---|---|
| Freestream conditions | $U_s, P_\infty, T_\infty$ | Select |
| Ideal equilibrium conditions | $T_2, \varepsilon_2$ | Shock tube charts[15] |
| Thick source function<br>Thick radiative $X$-section | $S_{T_s}, \sigma_T$ | Obtain from Fig. 4 at assumed electron temperature (typically $T_2$) |
| Thin source function<br>Thin radiative $X$-section | $S_t, \sigma_t$ | Obtain from Fig. 4 at $T_2$ |
| Thin exponent | $n$ | 3–5 |
| Gas properties | $MW, h_A^0, h_I^0$, etc. | Select |
| Relaxation length | $X_R$ | Fig. 5 |
| Correlation parameter | $B$ | $B = \dfrac{4.62\bar{h}_2}{K_{Ts}(\bar{h}_2+1)X_R}$ |

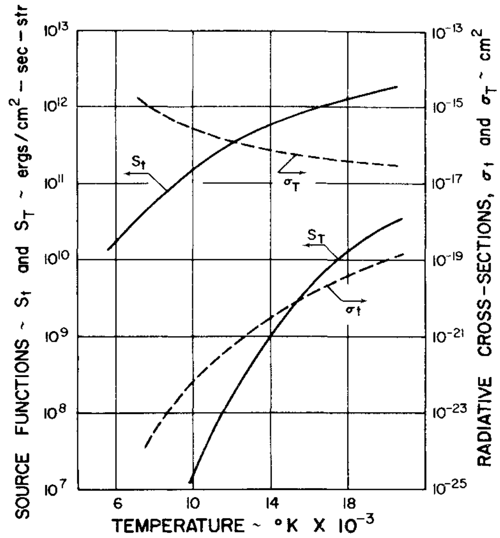


Fig. 4 Radiative properties of high temperature air.

dimensional $\bar{h}$ associated with the ideal postshock equilibrium conditions. This formula was determined in this study and has been found to yield results in agreement with experiment.[9]

On Fig. 4 the thick radiative properties are based[8] upon nitrogen in the vacuum ultraviolet (620–1100 Å), and they should be selected in accordance with the value assumed for the average electron temperature in the relaxation zone. The radiative cross section, $\sigma_T$, is an average value for the region, but the indicated source function is only one-tenth of the corresponding black body function. This decrease is included in order to approximately account for the nonequilibrium correction [see Eq. (4)] required in the VUV, and it is based on the fact that the average correction factor for the results on Fig. 2 was 0.16. While the actual correction factor varies from zero to one in the nonequilibrium zone, it is felt that the use of an average value is in keeping with the spirit of the present approximate analysis. If anything, a correction factor of 0.10 will underestimate radiative losses since line radiation may also be contributing to the loss near the shock front.

The curves for the thin radiative properties, $\sigma_t$ and $S_t$, are for equilibrium nitrogen radiation from the visible portion of the spectrum (1570–7870 Å), and it is sufficiently accurate to base them upon the ideal equilibrium temperature. It should be noted that for the conditions considered here that nitrogen radiative properties have been shown to be accurate representations of air properties.[8] In all cases $K_{Ts}$ and $K_{t0}$ can be adequately computed via $K_{Ts} = N_{As}\sigma_T$ and $K_{t0} = N_{A2}\sigma_t$ where $N_{A2}$ is

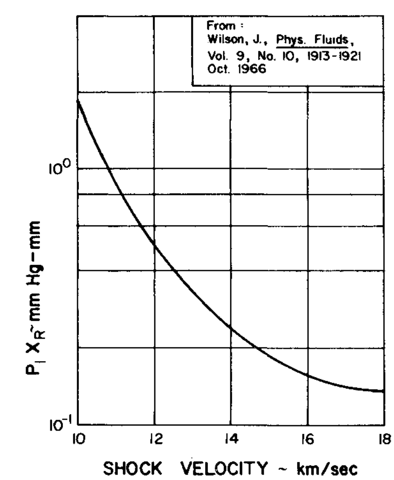


Fig. 5 Relaxation distance for shock waves in air.

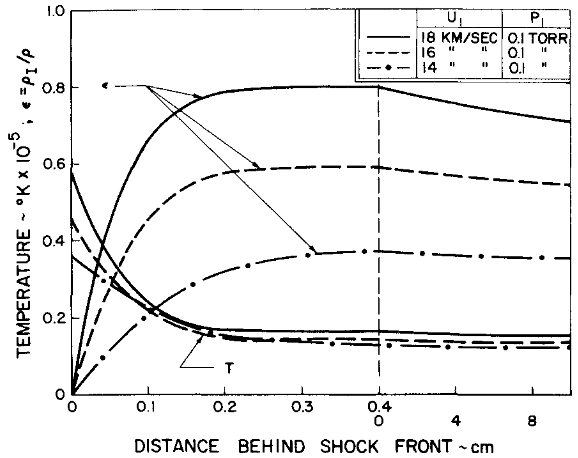


Fig. 6 Typical air normal shock solutions (initial $T_e = T_2$).

based upon ideal equilibrium. Likewise, $E_{t0}$ can be computed using only the first term of Eq. (8).

The preceding approach and solutions have been used for a series of parametric studies of air normal shock waves between 14–18 km/sec and for initial pressures ranging from 0.10 torr up to 1.0 torr. Some of the results are discussed next.

## Discussion of Results

Some typical solutions obtained with the preceding approach for air normal shock waves are shown on Fig. 6. These results can be obtained by hand or in about 0.6 sec using a WATFIV computer program (IBM 360/65). Notice that the horizontal scale is different for the thick and thin regions, which are separated by a dashed vertical line, and that the degree of ionization profiles have the same shape as that exhibited by the semidetailed calculations on Fig. 2. The latter tends to substantiate the use of the approximation given by Eq. (10).

For the three velocities indicated on Fig. 6, the solutions all show the same pattern. From a relatively high temperature near the shock front, the flow cools rapidly due primarily to chemical relaxation to some equilibrium value. After that radiative cooling from the visible region becomes important. This is exhibited in the thin region by a slow decrease in the temperature and also, perhaps more vividly, by a decrease in the degree of ionization. The latter is particularly sensitive in the equilibrium region to even slight changes in temperature. The solutions were terminated at 10 cm simply for convenience.

Unfortunately no detailed solutions or experimentally determined profiles for nonequilibrium reacting radiating air normal shock wave in this velocity range are known, but comparison with solutions in other gases indicate that the present results are qualitatively correct. Also these solutions do yield relaxation distances in accord with experiment,[9] and the correct conditions for the equilibrium region.[15]

In order to test the flexibility of the present solution technique several comparative and parametric studies were conducted. Figure 7 shows temperature profiles in the nonequilibrium region obtained including and excluding thermal conduction. (Similar results were also obtained at 14 km/sec.) Notice the large differences in temperature throughout the relaxation region and in particular at the shock front. It is believed that this is the first time thermal conduction in the nonequilibrium region behind a hypervelocity shock has been investigated, and it is obvious that it may be important and that possibly it should be included in solutions. Unfortunately, experimental verification of the importance of thermal conduction may be difficult to obtain since the effect is primarily associated with the heavy particle temperature. The electron temperature and relaxation distance are essentially the same for the two cases.

Parametric studies of the effect of the value of the thick radiative cross section, $\sigma_T$, were also conducted. Variations up to a factor of ten were considered; but no significant effect on the shock structure was detected, thus indicating that the flow in the nonequilibrium region is relatively insensitive to the value of $\sigma_T$ and primarily chemistry dominated. This does not mean, however, that radiation has no effect in the thick region. For the curves shown on Fig. 6, the temperature at the end of the thick zone was, due to radiative cooling, typically 0.5–1.5% below the ideal Rankine-Hugoniot equilibrium conditions while the degree of ionization was typically 4–8% lower.

A similar study was conducted on the effect of the thin radiative cross section and on the value of the exponent, $n$, used in Eq. (14). For the latter, values of three and five were tried, and the difference in the thin flowfield region amounted to less than $\frac{1}{2}$%. On the other hand, Fig. 8 shows that the value for the thin radiative absorption cross section has a strong effect on the equilibrium zone properties. As can be seen, a factor of ten increase causes not only significant radiative cooling but also

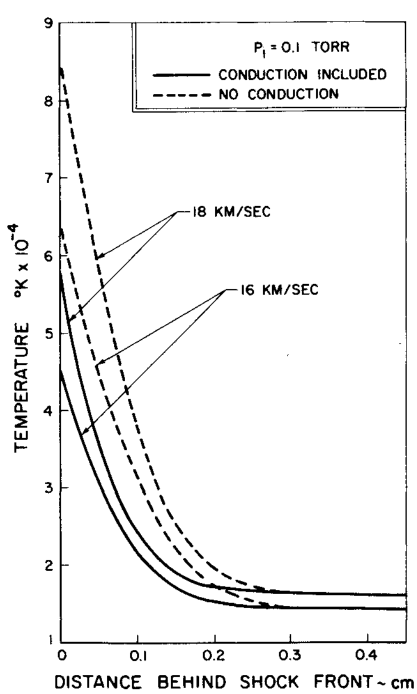


Fig. 7 The effect of thermal conduction on relaxation zone temperature.

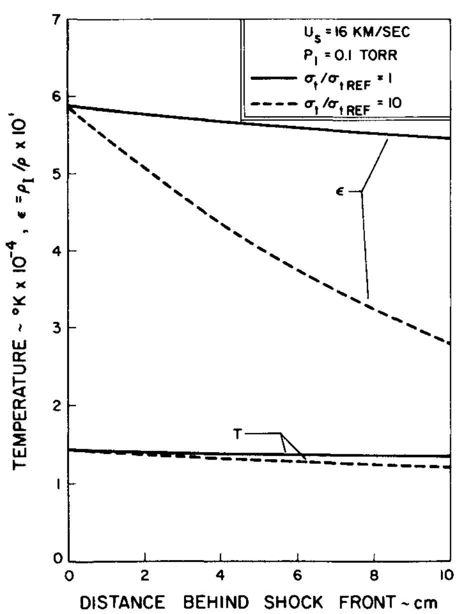


Fig. 8 The effect of the thin radiative absorption cross section on equilibrium zone properties.

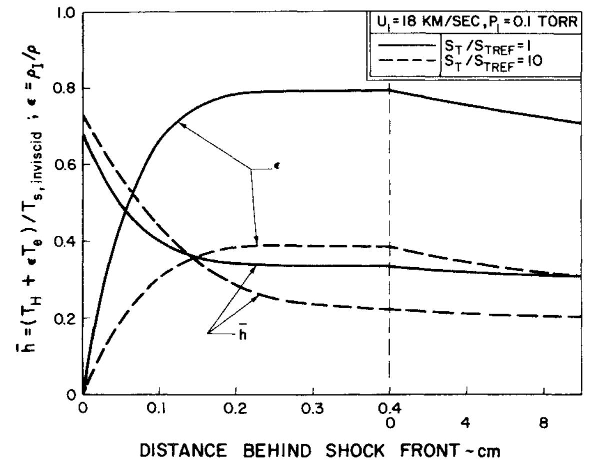


**Fig. 9 The effects of the thick radiative source function on shock layer profiles.**

a large change in the chemical composition, which is very sensitive to temperature.

It should be noted that the equilibrium results of the present study, such as those on Fig. 8, are in general agreement with those of Chien and Compton,[16] although the present values are slightly higher. This trend is to be expected since the present results are only one-dimensional while those of Ref. 16 include radiative losses to sidewalls.

Figure 9 shows the effect of a factor of ten increase in the thick source function. Such an increase could result (see Fig. 4) from assuming an average nonequilibrium electron temperature of 18,000°K instead of 15,000°K. As indicated in the discussion of Fig. 1, a nonequilibrium electron temperature higher than the ideal equilibrium temperature probably should be assumed if the experimentally observed relaxation lengths[9] are to be reproduced by detailed calculations. Also, such enhanced electron temperatures have been predicted for other gases[2-4] by detailed solutions. While Fig. 1 shows the effect of a high electron temperature on a radiatively uncoupled flowfield, Fig. 9 shows the effect with radiative-gasdynamic coupling included. Near the shock front, the effect on the nondimensional enthalpy is small. Downstream, however, the effect is large. In particular, the temperature and the composition at the downstream end of the thick region are considerably different from the ideal Rankine-Hugoniot values of $\bar{h} = 0.35$ and $\varepsilon = 0.86$. Further, these differences subsequently affect the entire thin equilibrium region. Notice that not only does an increase in $S_T$ (i.e., electron temperature) increase the radiative cooling but also that the cooling occurs almost entirely in the nonequilibrium zone.

Figure 9 indicates that the flowfield results are sensitive to the value assumed for the nonequilibrium zone electron temperature. Based upon these results and those of Refs. 2–6, it is suggested that for the present approximate solution $T_e$ be selected 10–15% above the ideal equilibrium temperature.

It should be pointed out that all of the present results are dependent upon the value used for the size of the relaxation region, and the values given on Fig. 5 have been disputed. In fact, some investigators maintain that for the present conditions the flowfield is completely frozen.[17] Thus, parametric studies concerning the effect of $X_R$ were conducted. In general, the nonequilibrium region was found to be always primarily chemistry dominated and no changes in the above conclusions were discovered. Nevertheless, it is believed that experimental studies of $X_R$, $T_e$, and $\varepsilon$ would be valuable, particularly if they had a time resolution of 0.05 μsec or better.

## Conclusions

Approximations applicable to radiating reacting hypervelocity shock waves have been investigated and a technique suitable for rapidly obtaining approximate solutions to such shock layers has been developed. This solution utilizes a coordinate system based upon the origin of the radiative losses and includes in a qualitatively correct manner the effects of chemical and thermal nonequilibrium, nongray radiative transfer, and thermal conduction. It has been applied to normal shock flows and the following has been determined.

1) Rapid, reasonably accurate solutions are possible.

2) For the conditions investigated, the flow near the shock front is a) primarily chemistry dominated, b) relatively insensitive to the thick radiative absorption cross section, c) sensitive to the magnitude of the thick radiative source function and nonequilibrium electron temperature. Radiative cooling can occur in the nonequilibrium zone and affect the equilibrium flow downstream.

3) Thermal conduction effects are significant in the region immediately behind the shock front.

It is believed that the solution techniques demonstrated in this paper could be incorporated into other viscous solution methods[18] and could be extrapolated to multidimensional and entry body flowfields.

## References

[1] Anderson, J. D., Jr., "An Engineering Survey of Radiating Shock Layers," *AIAA Journal*, Vol. 7, No. 9, Sept. 1969, pp. 1665–1675.

[2] Nelson, H. F. and Goulard, R., "Structure of Shock Waves with Nonequilibrium Radiation and Ionization," *The Physics of Fluids*, Vol. 12, No. 8, Aug. 1969, pp. 1605–1617.

[3] Chapin, C. E., "Nonequilibrium Radiation and Ionization in Shock Waves," AA&ES 67-9, June 1967, Purdue Univ., Lafayette, Ind.

[4] Foley, W. H. and Clarke, J. H., "Shock Wave Structured by Nonequilibrium Ionizing and Thermal Phenomena," *The Physics of Fluids*, Vol. 16, No. 3, March 1973, pp. 373–383.

[5] Carlson, L. A., "Radiative-Gasdynamic Coupling and Nonequilibrium Effects behind Reflected Shock Waves," *AIAA Journal*, Vol. 9, No. 5, May 1971, pp. 858–865.

[6] Carlson, L. A., "Radiative Cooling and Nonequilibrium Chemistry Coupling behind Normal Shock Waves," *AIAA Journal*, Vol. 10, No. 2, Feb. 1972, pp. 230–232.

[7] Skoczlas, K. A., "An Evaluation of Simplified Methods of Computing Radiating-Chemically Reacting Flowfields," Rept. TAMRF-711-7203, May 1972, Texas Engineering Experimental Station, College Station, Texas.

[8] Knott, P. R., Carlson, L. A., and Nerem, R. M., "A Further Note on Shock Tube Measurements of End-Wall Radiative Heat Transfer in Air," *AIAA Journal*, Vol. 7, No. 11, Nov. 1969, pp. 2170–2172.

[9] Wilson, J., "Ionization Rate of Air Behind High Speed Shock Waves," *The Physics of Fluids*, Vol. 9, No. 10, Oct. 1966, pp. 1913–1921.

[10] Olstad, W. B., "A Thick Thin Approximation for Radiative Transfer," AIAA Paper 73-715, Palm Springs, Calif., 1973.

[11] Carlson, L. A., "A Radiating-Conducting Thick-Transparent Normal Shock Solution," *The Physics of Fluids*, Vol. 15, No. 12, Dec. 1972, pp. 2150–2152.

[12] Cheng, H. K., *Fundamental Phenomena in Hypersonic Flow*, edited by J. G. Hall, Cornell Univ. Press, Ithaca, N.Y., 1966, p. 90.

[13] Schneider, W., "Effect of Radiation on Hypersonic Stagnation Flow at Low Density," *Zeitschrift Fur Flugwissenschaften*, Vol. 18, Nos. 2–3, Feb. 1970, pp. 50–58.

[14] Neel, C. A. and Lewis, C. H., "Interpolations of Imperfect Air Thermodynamic Data II. At Constant Pressure," AEDC-TDR-64-184, Sept. 1964, Arnold Engineering Development Center, Tullahoma, Tenn.

[15] Laird, J. D. and Heron, K., "Shock Tube Gas Dynamic Charts, Part I," RAD-TM-64-12, April 1964, Avco Corp., Wilmington, Mass.

[16] Chien, K. Y. and Compton, D. L., "Radiative Cooling of Shock-Heated Air in Cylindrical Shock Tubes," *AIAA Journal*, Vol. 8, No. 10, Oct. 1970, pp. 1896–1898.

[17] Schneider, W., "Interaction of Thermal Radiation with the Flow in a Viscous Shock Layer," DLR-FB-71-89, Oct. 1971, DVLR, Aachen, W. Germany.

[18] Jischke, M. C., "Asymptotic Solution for Viscous, Absorbing, Emitting Shock Layer," *AIAA Journal*, Vol. 9, No. 10, Oct. 1971, pp. 1920–1928.